PAGEOPH, Vol. 130, No. 1 (1989)

0033-4553/89/010031-15$1.50 + 0.20/0

Relationship Between Thermally Forced Surface Wind and Sea Surface Temperature Gradient

P. C. CHU[1]

Abstract—An important part of the influence of the oceans on the atmosphere is through direct radiation, sensible heat flux, and release of latent heat of evaporation, whereby all of these processes are directly related to the surface temperature of the oceans. A main effect of the atmosphere on the oceans is through momentum exchange at the air-ocean interface, and this process is directly related to the surface wind stress. The sea surface temperature (SST) and the surface wind stress are the two important components in the air-ocean system. If SST is given, a thermally forced boundary layer atmospheric circulation can be simulated. On the other hand, if the surface wind stress is given, the wind-driven ocean waves and ocean currents can be computed.

The relationship between SST and surface wind is a coupling of the atmosphere and the oceans. It changes a one-way effect (ocean mechanically driven by atmosphere, or atmosphere thermally forced by oceans) into two-way air-sea interactions. Through this coupling the SST distribution, being an output from an ocean model, leads to the thermally forced surface winds, which feeds back into the ocean model as an additional forcing.

Based on Kuo's planetary boundary layer model, a linear algebraic equation is established to link the SST gradient with the thermally forced surface wind. The surface wind blows across the isotherms from cold to warm region with some deflection angle α to the right (left) in the Northern (Southern) Hemisphere. Results from this study show that the atmospheric stratification reduces both the speed and the deflection angle of the thermally forced wind, however, the Coriolis' effect increases the wind speed in stable atmosphere ($Ri > 10^{-4}$) and increases the deflection angle.

Key words: Air-sea interaction, atmospheric stratification, Coriolis effect, marine atmospheric boundary layer, sea surface temperature gradient, thermally forced surface wind.

1. Introduction

Since 1970 significant progress was made both in our ability to carry out air-sea interaction field work and in our understanding of many of the processes found on both sides of the air-sea interface. The observational air-sea interaction research is classified into three categories. The first type of experiments, designed to study the ocean responses to the atmospheric forcings, includes MILE (Mixed Layer Experiment) conducted near 50°N, 145°W for 20 days in April and September 1977 in

[1] Department of Oceanography, Naval Postgraduate School, Monterey, CA 93943, U.S.A.

Report Documentation Page

Form Approved
OMB No. 0704-0188

1. REPORT DATE **1989**	2. REPORT TYPE	3. DATES COVERED **00-00-1989 to 00-00-1989**

4. TITLE AND SUBTITLE **Relationship Between Thermally Forced Surface Wind and Sea Surface Temperature Gradient**	5a. CONTRACT NUMBER 5b. GRANT NUMBER 5c. PROGRAM ELEMENT NUMBER
6. AUTHOR(S)	5d. PROJECT NUMBER 5e. TASK NUMBER 5f. WORK UNIT NUMBER
7. PERFORMING ORGANIZATION NAME(S) AND ADDRESS(ES) **Naval Postgraduate School,Department of Oceanography,Monterey,CA,93943**	8. PERFORMING ORGANIZATION REPORT NUMBER
9. SPONSORING/MONITORING AGENCY NAME(S) AND ADDRESS(ES)	10. SPONSOR/MONITOR'S ACRONYM(S) 11. SPONSOR/MONITOR'S REPORT NUMBER(S)

12. DISTRIBUTION/AVAILABILITY STATEMENT
Approved for public release; distribution unlimited

13. SUPPLEMENTARY NOTES

14. ABSTRACT

15. SUBJECT TERMS

16. SECURITY CLASSIFICATION OF:			17. LIMITATION OF ABSTRACT	18. NUMBER OF PAGES	19a. NAME OF RESPONSIBLE PERSON
a. REPORT **unclassified**	b. ABSTRACT **unclassified**	c. THIS PAGE **unclassified**	**Same as Report (SAR)**	**15**	

Standard Form 298 (Rev. 8-98)
Prescribed by ANSI Std Z39-18

order to observe upper ocean responses to early-fall storms (DAVIS *et al.*, 1981a,b); LOTUS (Long-Term Upper Ocean Study) conducted from May 1982 to May 1984 with the same goal of examining the vertical structure of the oceanic response to atmospheric forcing (BRISCO and WELLER, 1984); the Research Platform FLIP (Floating Laboratory Instrument Platform) conducted off the coast of southern California in April and May of 1980 to obtain higher vertical resolution and more accurate measurement; and MILDEX (Mixed Layer Dynamics Experiment) centered on the FLIP and conducted in October and November of 1983 with the goal of collecting upper ocean data. These experiments are basically one-dimensional (in vertical) although information about the horizontal variability might be obtained from the MILDEX in addition to the detailed observation of the vertical structure. The second type of experiments, designed to study the transfer processes in the marine atmospheric boundary layer (MABL), includes aircraft measurements of MABL turbulence (GREENHUT and BEAN, 1981); AMTEX (Air Mass Transformation Experiment, February 1974 and February 1975) concentrated on the cold air from Asia moving across the warm Kuroshio Current off the coast of Japan; and GATE (GARP Atlantic Tropical Experiment) conducted near the equator in the Atlantic Ocean in the summer of 1974. The third type of experiments, designed to study the horizontal variability in both the ocean and the atmosphere and to investigate the two-way air-sea interactions, includes JASIN (Joint Air-Sea Interaction Experiment; POLLARD, 1978) conducted in the fall of 1978 in the Rockall Trough region between Scotland and Iceland; FASINEX (Frontal Air-Sea Interaction Experiment) conducted in February and March 1986 in the vicinity of 27°N, 70°W (STAGE and WELLER, 1985, 1986). Besides the two-way interaction task, FASINEX also dealt with the response of the upper ocean to atmospheric forcing in the oceanic front in the subtropical convergence zone southwest of Bermuda, and the response of the lower atmosphere in the vicinity of the oceanic front.

Through observational studies, it is recognized that surface wind and SST distribution are two important elements in the air-sea coupled system. Spatial variability in SST associated with an oceanic eddy causes mesoscale horizontal variability in the fluxes of momentum and moisture in the MABL (GUYMER *et al.*, 1983), which changes the atmospheric circulation in the MABL. However, the surface wind, acting through stress, mechanically generates the ocean currents and waves, and redistributes the SST (CHU, 1986). Therefore, it is important, in the air-sea coupled system, to establish a relationship between the SST distribution and the thermally forced surface wind. In the subsequent sections the symbol ~ denotes nondimensional variables.

2. *Thermally Forced Boundary Layer Air Flow*

In this section a K-closure planetary boundary layer (PBL) atmospheric model treated by KUO (1973) and CHU (1986, 1987a,b,c) is utilized to simulate thermally

forced boundary layer air flow. KUO (1973) successfully separated the forcings of the PBL air flow into two parts: mechanical forcing (geostrophic wind) at the top of the PBL and the thermal forcing at the surface. In this paper we only deal with the thermal forcing. The vertical diffusion coefficient is made a simple function of static stability. In regions of stable stratification the vertical diffusion coefficient is taken as a constant (ROBINSON and STOMMEL, 1959). The coordinate system is chosen such that the x-axis is in the cross-isotherm direction (pointing into the direction of increasing temperature) and the y-axis parallels the isotherms, as shown in Figure 1. It is considered that spatial variations are much larger perpendicular to the isotherms than parallel to them, and hence derivatives with respect to y are assumed to be zero.

The air potential temperature is divided into two parts: a basic state $\theta_B(z)$ and perturbation θ'.

The basic state is assumed to be a linear function of z:

$$\theta_B(z) = \theta_{B0} + \left(\frac{N^2\theta_{B0}}{g}\right)z \tag{1}$$

where θ_{B0} is a basic air potential temperature at the surface, and N the Brunt-Väisälä frequency. The effort of this research is to model the thermally forced circulation; therefore, the surface temperature perturbation $\theta'|_{z=0}$ is given as a known function, which can be expanded into Fourier sine series in x-direction. Since we define here a linear system, there is no loss of generality to assume that the surface temperature perturbation only contains the first component:

$$\theta'|_{z=0} = \left(\frac{LG_T}{\pi}\right)\sin\left(\frac{\pi x}{L}\right) \tag{2}$$

where G_T is the characteristic surface temperature gradient, and L is the width of surface thermal inhomogeneity. The surface wind blows across the isotherms from a cold to warm surface with some deflection angle α to the right (left) in the Northern (Southern) Hemisphere (Figure 1). The coordinates and variables are nondimensionalized by setting

$$\begin{gathered}(x, z) = (\tilde{x}L, \tilde{z}\delta),\\ \frac{\theta'}{\theta_{B0}} = \left(\frac{G_T L}{\theta_{B0}}\right)\tilde{\theta},\\ (u, v, w) = U\left(\tilde{u}, \tilde{v}, \frac{\tilde{w}\delta}{L}\right),\\ \delta = (\nu/\Omega)^{1/2}\end{gathered} \tag{3}$$

where ν is the vertical eddy viscosity, Ω is the angular velocity of the earth's rotation, δ is the Ekman depth of the atmosphere, and

$$U \equiv \frac{g\delta G_T}{2\Omega\theta_{B0}} \tag{4}$$

is the scale of thermally forced surface wind. We assume that the local air flow satisfies the modified Boussinesq approximation (KUO, 1973), and has the simplest form of dissipation namely, Rayleigh friction with decay rate, R, which is taken as a constant ($0.4 \times 10^{-1}\ \mathrm{s}^{-1}$) in the present study, and Newtonian cooling, also with decay rate, R. The vorticity equation, the momentum equation (both in the y direction), and the heat equation for the air disturbances generated by differential surface temperature gradient are (CHU, 1986, 1987a,b,c)

$$\left(E\frac{\partial^2}{\partial \tilde{z}^2}-\gamma\right)\frac{\partial^2\tilde{\psi}}{\partial \tilde{z}^2}=f_0\frac{\partial \tilde{v}}{\partial \tilde{z}}-\frac{\partial \theta}{\partial \tilde{x}}, \tag{5}$$

$$\left(E\frac{\partial^2}{\partial \tilde{z}^2}-\gamma\right)\tilde{v}=-f_0\frac{\partial \tilde{\psi}}{\partial \tilde{z}}, \tag{6}$$

$$\left(E\frac{\partial^2}{\partial \tilde{z}^2}-\gamma\right)\tilde{\theta}=Ri\frac{\partial \tilde{\psi}}{\partial \tilde{x}}. \tag{7}$$

In the foregoing,

$$\tilde{u}=-\frac{\partial\tilde{\psi}}{\partial \tilde{z}},\quad \tilde{w}=\frac{\partial\tilde{\psi}}{\partial \tilde{x}},\quad \gamma=\frac{R}{2\Omega} \tag{8}$$

where $f_0=\sin\phi$, is the nondimensional Coriolis parameter, ϕ is the latitude, and

$$E\equiv\frac{\nu}{2\Omega\delta^2}=\frac{1}{2},\quad Ri\equiv\left(\frac{\delta N}{2L\Omega}\right)^2 \tag{9}$$

are the Ekman and Richardson numbers, respectively. Eliminating $\tilde{v}$ and $\tilde{\theta}$ from (5)–(7) we find that the streamfunction satisfies the following partial differential equation:

$$\left(\frac{1}{4}\frac{\partial^4}{\partial \tilde{z}^4}-\gamma\frac{\partial^2}{\partial \tilde{z}^2}+\gamma^2+f_0^2\right)\frac{\partial^2\tilde{\psi}}{\partial \tilde{z}^2}+Ri\frac{\partial^2\tilde{\psi}}{\partial \tilde{x}^2}=0. \tag{10}$$

We solve (10) for the streamfunction $\tilde{\psi}$, and obtain the solutions of $\tilde{v}$ and $\tilde{s}$ from (6) and (7) after substituting $\tilde{\psi}$. The boundary conditions in the vertical direction are derived as follows. The dependent variables should remain finite as $z\to\infty$, i.e.,

$$\lim_{z\to\infty}\left(|\tilde{\psi}|,\left|\frac{\partial\tilde{\psi}}{\partial \tilde{z}}\right|,|\tilde{v}|,|\tilde{s}|\right)<\infty. \tag{11a}$$

The surface boundary conditions are:

$$\tilde{\psi}|_{z=0}=0 \tag{11b}$$

which is the kinematic condition, indicating no airflow can cross the surface

$$\tilde{\theta}|_{z=0}=\frac{\sin\pi\tilde{x}}{\pi} \tag{11c}$$

which is the same as the surface thermal condition (2). From the two equivalent forms of the surface stress

$$\vec{\tau}|_{z=0} = \rho_a C_D |V_a| (u\vec{i} + v\vec{j})|_{z=0},$$
$$\vec{\tau}|_{z=0} = \rho_a v \frac{\partial}{\partial z}(u\vec{i} + v\vec{j})|_{z=0}$$

we have (after nondimensionalization)

$$\left(\frac{\partial \tilde{\psi}}{\partial \tilde{z}} - M \frac{\partial^2 \tilde{\psi}}{\partial \tilde{z}^2}\right)\bigg|_{\tilde{z}=0} = 0, \tag{11d}$$

$$\left(\tilde{v} - M \frac{\partial \tilde{v}}{\partial \tilde{z}}\right)\bigg|_{\tilde{z}=0} = 0 \tag{11e}$$

which indicate the surface slip conditions for $\tilde{u}$ (i.e., $\partial\tilde{\psi}/\partial\tilde{z}$) and $\tilde{v}$. Here

$$M = \frac{v}{C_D |V_a| \delta}, \tag{12a}$$

is a measure of the effective depth of the constant stress-sublayer (KUO, 1973), and C_D is the air drag coefficient. V_a is a characteristic speed for the large scale surface wind (including the mechanically driven part) and taken as 10 m s^{-1}. We define the dimensional drag coefficient as

$$C_D^* = C_D |V_a| \tag{12b}$$

therefore

$$M = \frac{v}{C_D^* \delta}. \tag{12c}$$

In the model M is taken as a known parameter. The heat equation (7) shows that the horizontal gradient of $\tilde{\psi}$ in the x-direction has the same form of variation as $\tilde{\theta}$, therefore, the streamfunction should be written as

$$\tilde{\psi}(\tilde{x}, \tilde{z}) = \eta(\tilde{z}) \cos \pi\tilde{x}. \tag{13}$$

Substituting (13) into (10) we obtain the following sixth order ordinary differential equation for η

$$\frac{d^6\eta}{d\tilde{z}^6} - 4\gamma \frac{d^4\eta}{d\tilde{z}^4} + 4(f_0^2 + \gamma^2)\frac{d^2\eta}{d\tilde{z}^2} - 4\pi^2 Ri \quad \eta = 0. \tag{14}$$

The solution of (14), which satisfies the top boundary conditions, has the following form

$$\eta(\tilde{z}) = \sum_{j=1}^{3} a_j \exp(\lambda_j \tilde{z}), \tag{15}$$

where the eigenvalues λ_j ($j = 1, 2, 3$) are the roots with negative real parts of the sixth order algebraic equation:

$$\lambda^6 - 4\gamma\lambda^4 + 4(f_0^2 + \gamma^2)\lambda^2 - 4\pi^2 Ri = 0 , \tag{16}$$

which shows that the eigenvalues λ_j ($j = 1, 2, 3$) are functions of the Richardson number, Ri, and sine of the latitude, f_0. Substituting (15) into (13) we obtain the streamfunction

$$\tilde{\psi}(\tilde{x}, \tilde{z}) = \sum_{j=1}^{3} a_j \exp(\lambda_j \tilde{z}) \cos \pi\tilde{x} \tag{17}$$

where a_1, a_2 and a_3 are integral constants. Integrating the momentum equation (6) and the heat equation (7) with respect to $\tilde{z}$ after substituting (17), we find that $\tilde{v}$ and $\tilde{s}$ are given by (CHU, 1986)

$$\tilde{v}(\tilde{x}, \tilde{z}) = \left[b \exp(-\sqrt{2\gamma}\tilde{z}) - 2f_0 \sum_{j=1}^{3} \frac{a_j\lambda_j \exp(\lambda_j \tilde{z})}{\lambda_j^2 - 2\gamma} \right] \cos \pi\tilde{x} , \tag{18}$$

$$\tilde{\theta}(\tilde{x}, \tilde{z}) = \left[-\frac{\sqrt{2\gamma} f_0 b}{\pi} \exp(-\sqrt{2\gamma}\tilde{z}) + 2\pi Ri \sum_{j=1}^{3} \frac{a_j}{\lambda_j^2} - 2\gamma \exp(\lambda_j \tilde{z}) \right] \sin \pi\tilde{x} \tag{19}$$

where b is also an integral constant. Substituting the solutions (17)–(19) into the surface boundary conditions listed in (11b,c,d,e) we obtain the following four algebraic equations for a_j and b

$$\sum_{j=1}^{3} a_j = 0 , \tag{20}$$

$$\sum_{j=1}^{3} \lambda_j (1 - M\lambda_j) a_j = 0 , \tag{21}$$

$$-2f_0 \sum_{j=1}^{3} \left[\frac{\lambda_j (1 - M\lambda_j)}{\lambda_j^2 - 2\gamma} \right] a_j + b(1 + \sqrt{2\gamma}) = 0 , \tag{22}$$

$$2\pi Ri \sum_{j=1}^{3} \frac{a_j}{\lambda_j^2 - 2\gamma} - \frac{\sqrt{2\gamma} f_0 b}{\pi} = \frac{1}{\pi} . \tag{23}$$

This set of linear algebraic equations implies that the integral constants a_1, a_2, a_3, and b depend on the Richardson number, Ri, on the sine of the latitude, f_0, and on the eigenvalues λ_1, λ_2, λ_3 (which are functions of Ri and f_0). Therefore, a_1, a_2, a_3, and b are functions of Ri and f_0. After the four constants a_1, a_2, a_3, and b are obtained by solving the four linear nonhomogeneous algebraic equations, we get the solutions of $\tilde{\psi}$, $\tilde{v}$, and $\tilde{\theta}$ from (17)–(19).

The thermally driven surface wind (dimensional form) is computed by

$$u|_{z=0} = U \operatorname{Re}\left(\frac{\partial \tilde{\psi}}{\partial \tilde{z}} \Big|_{\tilde{z}=0} \right) \cos \pi\tilde{x}, \quad v|_{z=0} = U \operatorname{Re}(\tilde{v}|_{\tilde{z}=0}) \cos \pi\tilde{x} \tag{24}$$

where Re( ) refers to the real part of a complex variable. Substituting (17) and (18) into (24) we have

$$u|_{z=0} = u_0 \cos \pi\tilde{x}, \quad v|_{z=0} = v_0 \cos \pi\tilde{x} , \tag{25}$$

where

$$u_0 \equiv U\,\mathrm{Re}\left(\sum_{j=1}^{3} a_j\lambda_j\right). \tag{26}$$

$$v_0 \equiv U\,\mathrm{Re}\left[b - 2f_0 \sum_{j=1} \frac{a_j\lambda_j}{\lambda_j^2 - 2\gamma}\right]. \tag{27}$$

The vector forms of the thermally forced surface wind and the SST gradient are given by

$$\vec{V} = (\vec{i}\,u_0 + \vec{j}\,v_0)\cos\pi\tilde{x}, \quad \nabla\theta|_{z=0} = \vec{i}\,G_T\cos\pi\tilde{x}\,. \tag{28}$$

It is noticed that $\vec{V}$ is to the right (left) of $\nabla\theta|_{z=0}$ in the Northern (Southern) Hemisphere, therefore

$$\vec{V} = \kappa\mu\begin{bmatrix}\cos\alpha & -\sin\alpha\\ \sin\alpha & \cos\alpha\end{bmatrix}\nabla\theta|_{z=0} \tag{29}$$

where

$$\kappa \equiv \frac{U}{G_T} = \frac{g\delta}{2\Omega\theta_{B0}} \tag{30a}$$

is the scale for the surface wind thermally driven by unit SST gradient;

$$\alpha \equiv \tan^{-1}\left(\frac{u_0}{v_0}\right) \tag{30b}$$

is the deflection angle (angle between $\vec{V}$ and $\nabla\theta|_{z=0}$); and

$$\mu \equiv \frac{\sqrt{u_0^2 + v_0^2}}{U} \tag{30c}$$

is the nondimensional thermally driven surface wind speed.

Table 1 lists the parameter values for the present calculations. By using them we compute the scale of the thermally forced surface wind

$$\mu = \frac{0.55(\mathrm{m/s})}{1(^\circ\mathrm{K}/100\ \mathrm{km})} \tag{31}$$

which is consistent with SCHMIDT's (1947) results that for a maximum land-water temperature gradient of 4.3°K/100 km, a maximum landbreeze intensity of about 2 m s^{-1} would be reached.

Table 1

The standard model parameters

$\theta_{B0} = 288^\circ$K,	$C_D^* = 0.01$ ms^{-1},	$\nu = 5$ m^{2}s^{-1}
$\Omega = 0.7282 \times 10^{-4}$ s^{-1},	$g = 9.81$ ms^{-2},	$R = 0.4 \times 10^{-4}$ s^{-1}.

3. Air Deflection Angle

The deflection angle α shown in Figure 1 is computed from (30b). Substituting (26) and (27) into (30b) we obtain

$$\alpha = \tan^{-1}\left\{\frac{\mathrm{Re}\left(\sum a_j\lambda_j\right)}{\mathrm{Re}\left[b - 2f_0\sum \frac{a_j\lambda_j}{\lambda_j^2 - 2\gamma}\right]}\right\}. \tag{32}$$

Equation (32) further shows that the direction of the thermally forced surface wind, α, does not change with the SST gradient. It depends on the eigenvalues λ_1, λ_2, λ_3, and on the integral constants a_1, a_2, a_3, b. We just mentioned that the eigenvalues and integral constants are the functions of Ri and f_0. Therefore, α is a function of Ri and f_0.

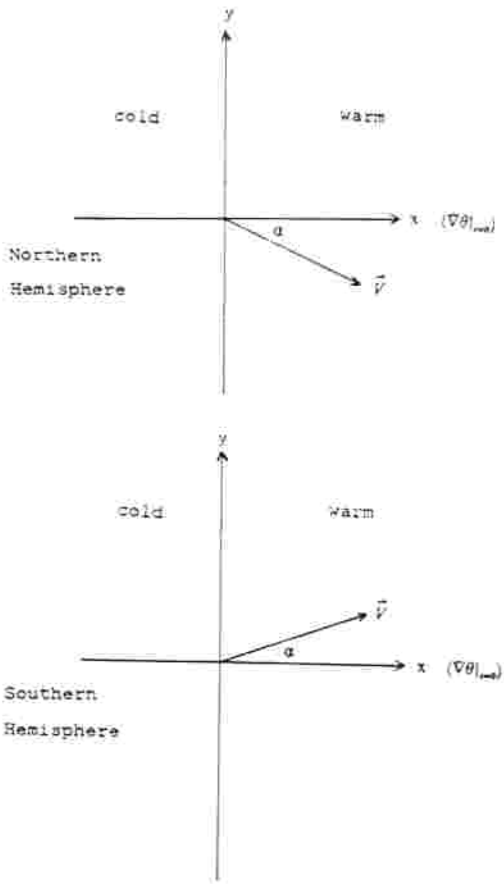

Figure 1
The coordinate system and the deflection angle α.

Figure 2 indicates the sensitivity of α on the latitude ϕ and on the logarithmic Richardson number $\log_{10}(Ri)$. The angle α increases with increasing latitude ϕ, and decreases with increasing Ri. It is seen that the two main factors (Coriolis' effect and atmospheric stratification) compete each other in such way that the earth rotation tends to deflect the thermally forced surface wind from the direction of SST gradient, however, the atmospheric stratification leads to reduce this deflection. In low latitude (weak Coriolis' effect) and strong stratified atmosphere, the deflection angle, α, is very small. Thermally forced surface wind blows nearly perpendicular to the isotherms from cold to warm regions. On the other hand, in high latitude (strong Coriolis' effect) and a weakly stratified atmosphere, the deflection angle, α, is large.

Figure 3a shows the α-$\log_{10}(Ri)$ curves for eight different latitudes ($\phi = 20°, 30°, \ldots, 90°$), whereas, Figure 3b displays the α-ϕ curves for five different values of the Richardson number ($\mathrm{Ri} = 10^{-6}, 10^{-5}, 10^{-4}, 10^{-3}$, and 10^{-2}). The curves in Figures 3a,b all reveal quadratic forms, however, difference can be found that the deflection angle α decreases with the increase of the stratification, and increases with increasing latitude. Taking ϕ and $\log_{10}(Ri)$ as two independent variables and using the regression method, we obtain the following formula for computing the deflection angle (in degrees):

$$\bar{\alpha} = 53.16 - 0.0038722(\phi - 90)^2 - 0.3419[\log_{10}(Ri) + 6]^2 . \tag{33}$$

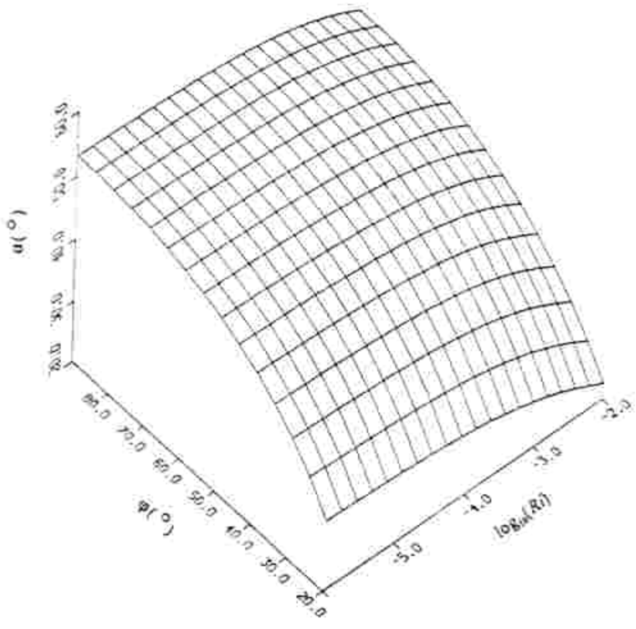

Figure 2
Dependence of α on latitude ϕ and the Richardson number Ri.

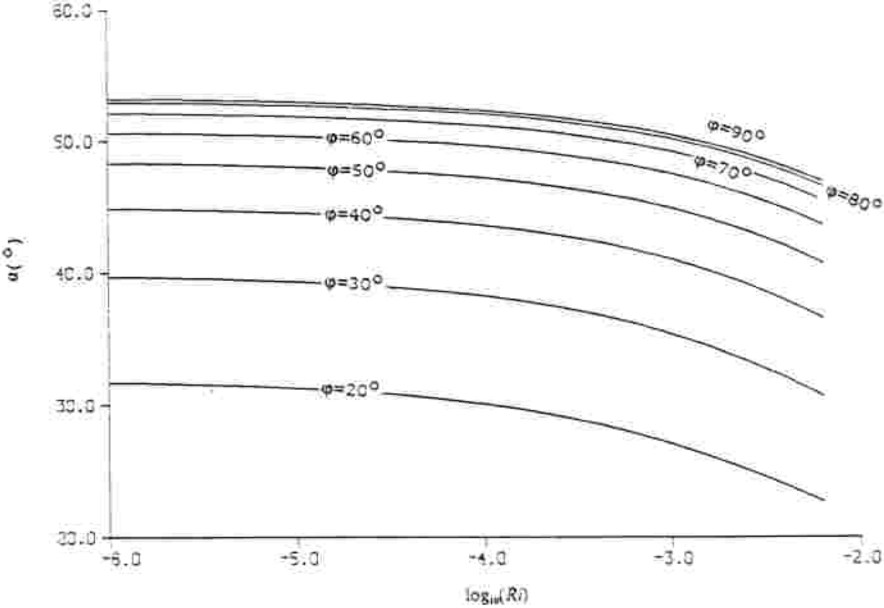

Figure 3a
α-$\log_{10}(Ri)$ curves for different latitudes.

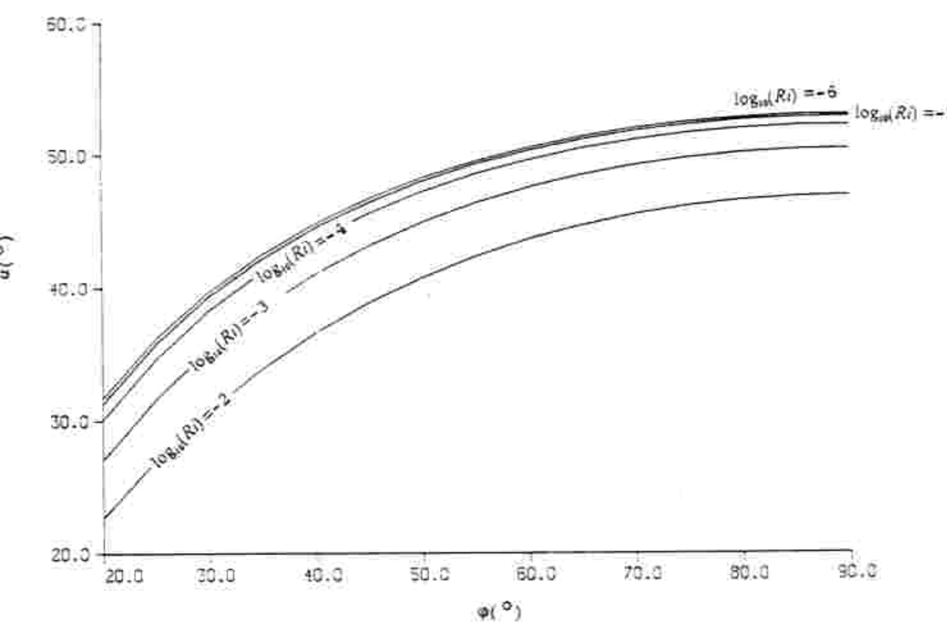

Figure 3b
α-ϕ curves for different Richardson numbers.

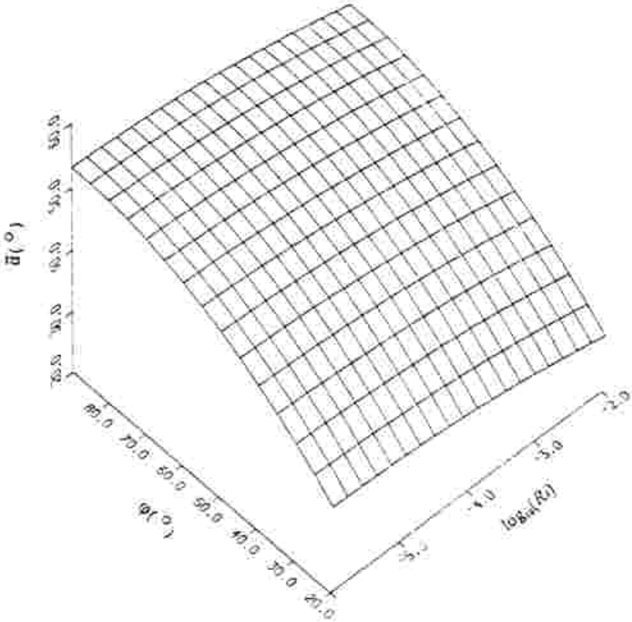

Figure 4
Dependence of estimated $\bar{\alpha}$ by (33) on latitude ϕ and the Richardson number Ri.

Figure 4 indicates the dependence of $\bar{\alpha}$ on ϕ and $\log_{10}(Ri)$. Comparing Figure 4 with Figure 2, we find that $\bar{\alpha}$ fits α quite well in most of the parameter space except for the low latitude ($\phi = 20°$) and a very stable atmosphere ($Ri = 10^{-2}$), where α overestimates the deflection angle by 5°.

4. *Thermally Forced Surface Wind Speed*

The maximum surface wind speed V_{max} is computed by

$$V_{max} = \sqrt{u_0^2 + v_0^2}. \tag{34}$$

Substituting (26) and (27) into (34) we get

$$V_{max} = U\mu \tag{35}$$

where μ is calculated by

$$\mu = \sqrt{\left[\mathrm{Re}\left(\sum a_j\lambda_j\right)\right]^2 + \left\{\mathrm{Re}\left[b - 2f_0 \sum \frac{a_j\lambda_j}{\lambda_j^2 - 2\gamma}\right]\right\}^2}. \tag{36}$$

The thermally driven surface wind speed is proportional to the SST gradient. Similar to the deflection angle α, the nondimensional speed μ is a function of Ri and $\sin\phi$. Figure 5 indicates the dependence of μ on ϕ and $\log_{10}(Ri)$. Figure 6a shows

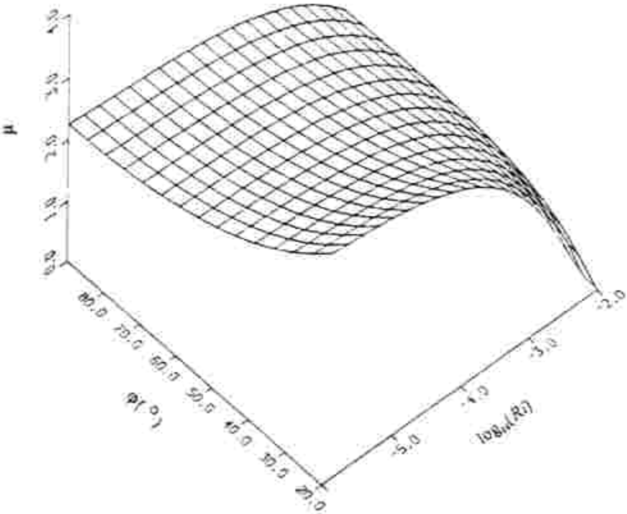

Figure 5
Dependence of μ on latitude ϕ and the Richardson number Ri.

the μ-$\log_{10}(Ri)$ curves for eight different latitudes, whereas, Figure 6b displays the μ-ϕ curves for five different values of the Richardson number. The sensitivity of μ on ϕ and on $\log_{10}(Ri)$ are different. The atmospheric stratification (Ri) is a diminishing factor for the thermally forced surface wind speed. The more stratified the atmosphere, the weaker the wind speed. However, the Coriolis' effect is more complicated than the stratification. For a stable atmosphere ($Ri > 10^{-4}$) the Coriolis' effect is an increasing factor; the higher the latitude, the stronger the wind is. Whereas for a less stable atmosphere ($Ri < 10^{-4}$) the Coriolis' effect is a diminishing factor, the higher the latitude, the weaker the wind is. Furthermore, the curves in Figure 6a reveal sinusoidal forms for the intensity parameter while Figure 6b displays hyperbolic forms. Using the regression method, we obtain the following formula for computing μ

$$\bar{\mu} = \frac{\cos\left\{\dfrac{\pi[\log_{10}(Ri) + 6]}{3.0716 \sin\phi + 6.568}\right\}}{0.2065 \sin\phi + 0.214}. \tag{37}$$

Figure 7 indicates the dependence of $\bar{\mu}$ on ϕ and $\log_{10}(Ri)$. Comparing Figure 7 with Figure 5, we find that $\bar{\mu}$ fits μ quite well in most areas of the parameter space except for low latitude ($\phi < 20°$).

If the atmospheric stratification and the location of the investigating area are given (i.e., Ri and ϕ are known), Equations (33) and (37) are employed to compute α and μ, and then Equation (29) is used to estimate the thermally forced surface wind driven by the SST gradient.

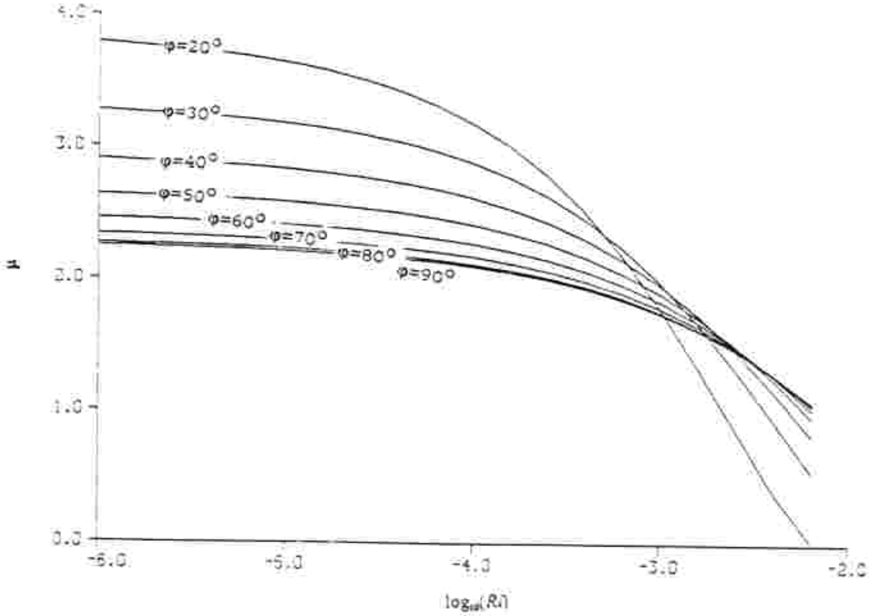

Figure 6a
μ-$\log_{10}(Ri)$ curves for different latitudes.

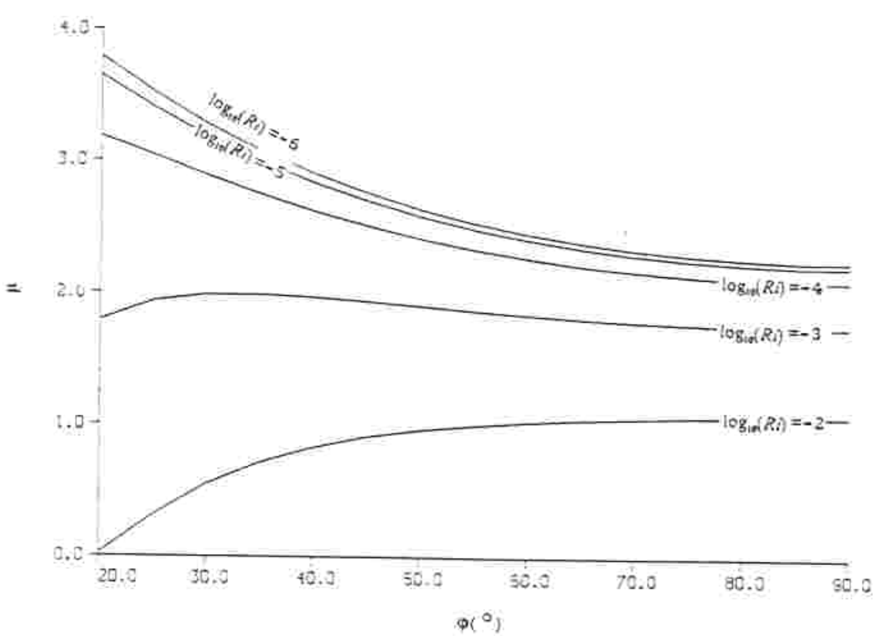

Figure 6b
μ-ϕ curves for different Richardson numbers.

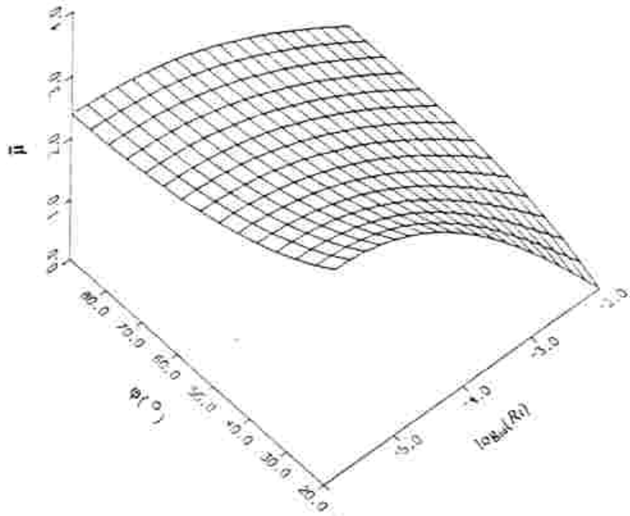

Figure 7
Dependence of estimated $\bar{\mu}$ by (37) on latitude ϕ and the Richardson number Ri.

5. *Conclusion*

(a) The formula (29) provides a useful coupling between the atmosphere and the ocean. If the thermally forced wind stress computed by this formula is added to the wind-driven ocean circulation models, the ocean model will be changed from a forced to a coupled one. We expect that it will have some applications to the air-sea interaction problems.

(b) The atmospheric stratification and Coriolis' effect are two main factors influencing the thermally driven surface wind. The stratification acts as a diminishing factor, reducing both the speed and the deflection angle. However, the Coriolis' effect is always an increasing factor for the deflection angle, whereas it is an amplifying factor for the wind speed if the atmosphere is quite stable ($Ri > 10^{-4}$), and is a diminishing factor for the wind speed if the atmosphere is less stable ($Ri < 10^{-4}$).

(c) The semi-empirical formulae for computing the deflection angle α and the nondimensional wind speed μ fit very well with the theoretical results except for the low latitude ($\phi = 20°$) and a very stable atmosphere. Therefore, these formulae are valid for middle and high latitudes ($\phi > 20°$).

(d) The formulae presented here are also valid for the thermally forced surface wind over land.

Acknowledgements

The author is grateful to Prof. H. L. Kuo of the University of Chicago and Prof.

R. W. Garwood, Jr. of the Naval Postgraduate School for invaluable discussion and comments. The reviewers' comments are also highly appreciated.

This research was supported by the Research Foundation Fund from the Naval Postgraduate School, and the Grant OCE 85–15400 from the National Science Foundation.

REFERENCES

BRISCO, M. G. and R. A. WELLER (1984), *Preliminary results from the Long-Term-Ocean Study (LOTUS)*. Dyn. Atmos. Ocean *8*, 243–265.

CHU, P. C. (1986), *An instability theory of ice-air interaction for the migration of the marginal ice zone*. Geophys. J. R. Astr. Soc. *86*, 863–883.

CHU, P. C. (1987a), *An instability theory of ice-air interaction for the formation of ice edge bands*. J. Geophys. Res. *92*, 6966–6970.

CHU, P. C. (1987b), *Generation of unstable modes of the iceward attenuating swell by ice breeze*. J. Phys. Oceanogr. *17*, 828–832.

CHU, P. C. (1987c), *An ice breeze mechanism for an ice divergence-convergence criterion in the marginal ice zone*. J. Phys. Oceanogr. *17*, 1627–1632.

DAVIS, R. E., R. DESZOEKE, D. HALPERN, and P. NIILER (1981a), *Variability in the upper ocean during MILE. Part I: The heat and momentum balances*. Deep-Sea Res. *28A*, 1427–1452.

DAVIS, R. E., R. DESZOEKE, and P. NIILER (1981b), *Variability in the upper ocean during MILE. Part II: Modelling the mixed layer response*. Deep-Sea Res. *28A*, 1453–1475.

GREEHUT, G. K. and B. R. BEAN (1981), *Aircraft measurements of boundary layer turbulence over the central equatorial Pacific Ocean*. Bound. Layer Meteor. *14*, 513–523.

GUYMER, T. H., J. A. BUSINGER, K. B. KATSAROS, W. J. SHAW, P. K. TAYLOR, W. G. LARGE, and R. E. PAYNE (1983), *Transfer processes at the air-sea interface*. Philos. Trans. R. Soc. London A. *308*, 253–273.

KUO, H. L. (1973), *Planetary boundary layer flow of a stable atmosphere over the globe*. J. Atmos. Sci. *30*, 53–65.

POLLARD, R. T. (1978), *The Joint Air-Sea Interaction Experiment-JASIN 1978*. Bull. Amer. Meteor. Soc. *59*, 1310–1318.

ROBINSON, A. R. and H. STOMMEL (1959), *The oceanic thermocline and the associated thermohaline circulation*. Tellus *11*, 295–308.

SCHMIDT, F. H. (1947), *An elementary theory of the land-and sea-breeze circulation*. J. Meteor. *4*, 9–15.

STAGE, S. A. and R. A. WELLER (1985), *The frontal air-sea interaction experiment (FASINEX); Part I: Background and scientific objectives*. Bull. Amer. Meteor. Soc. *66*, 1511–1520.

STAGE, S. A. and R. A. WELLER (1986), *The frontal air-sea interaction experiment (FASINEX); Part II: Experiment plan*. Bull. Amer. Meteor. Soc. *67*, 16–20.

(Received January 11, 1988, revised April 13, 1988, accepted June 4, 1988)